Effect of Distributor Designs on the Flow Development in Downer Reactor

Philip M. Johnston, Jing-Xu Zhu, Hugo I. de Lasa, and Hui Zhang
Chemical Reactor Engineering Centre, Dept. of Chemical and Biochemical Engineering, University of Western Ontario, London, Ontario, Canada, N6A 5B9

Cocurrent downflow circulating fluidized-bed (or downer) reactors have been proposed as a better alternative to upflow riser reactors for certain types of chemical reactions where a short contact time is required and the intermediate is the desired product, given the uniform flow structure and the greatly reduced gas and solids dispersion in the axial direction observed in the downers (Zhu et al., 1995; Wei and Zhu, 1996; Zhu and Wei, 1996). Characteristics of downer FCC reactors, for example, as stated in patent articles by Mobil and Texaco (Gross and Ramage, 1983; Gross, 1983; Niccum and Bunn, 1985), include a uniform distribution of catalyst, decreased contact time of catalyst with the feed and reduced coking.

Despite the advantages of downer reactors, there is a lack of understanding of gas and solids distribution, flow development, and solids acceleration in the entrance region. Past hydrodynamic studies have focused on specific regions within the downer, typically in the regions away from the distributors (Bai et al., 1991; Wang et al., 1992; Wei et al., 1994, 1995; Zhu et al., 1995; Herbert et al., 1994, 1997; Sobocinski et al., 1995). Since initial gas and solids distributions are extremely important for the short contact time reactions encountered in the downer, the mechanisms of the flow distribution, flow development, and acceleration must be more clearly understood. However, only very limited studies have been carried out to measure some rather isolated flow behaviors in the downer entrance region (Wei et al., 1996; Mirgain et al., 1998; Wirth and Schiewe, 1998) from which no firm conclusion can be drawn on the flow development and on the effects of the distributor design. The purpose of the present study is, therefore, to systematically study solids flow behavior in the downer entrance region with three types of distinctly different gas-solids distributor designs.

Experimental Equipment

All experiments were performed in the circulating fluidized-bed apparatus, shown in Figure 1. From the storage tank, solids fall through a butterfly valve into the bottom of the riser and then are entrained up the 15.1 m tall acrylic riser with a 0.1 m diameter. Solids are separated from the flowing air in the primary riser cyclone located at the downer top and are redistributed through a fluidized-bed solids distributor before entering the 9.3 m acrylic downer with smooth internal surface. After the downer, they are first separated from the carrying air in a quick inertial separator (with more than 99% efficiency). Most of the solids are further stripped from the flowing air in secondary and tertiary cyclones before

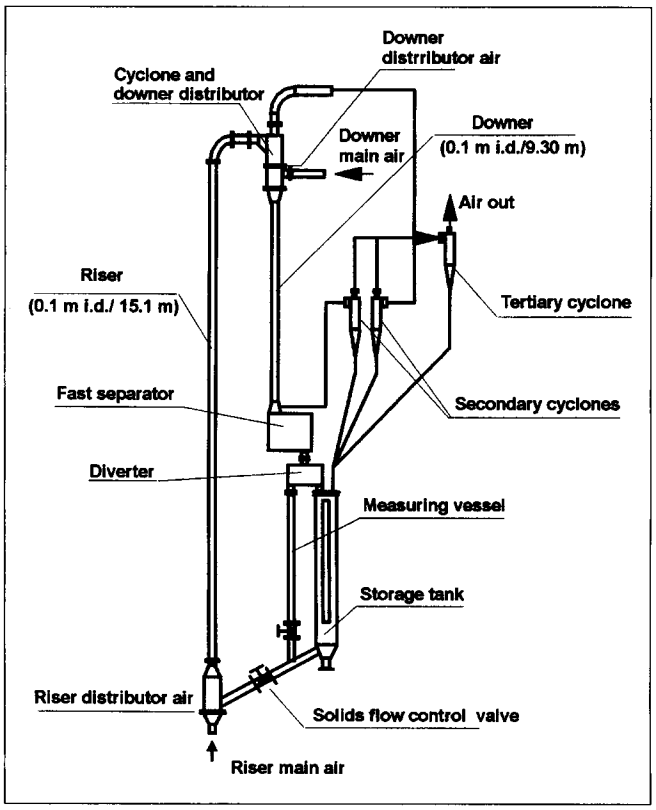

Figure 1. Downer and riser operating system.

Correspondence concerning this article should be addressed to J. Zhu.

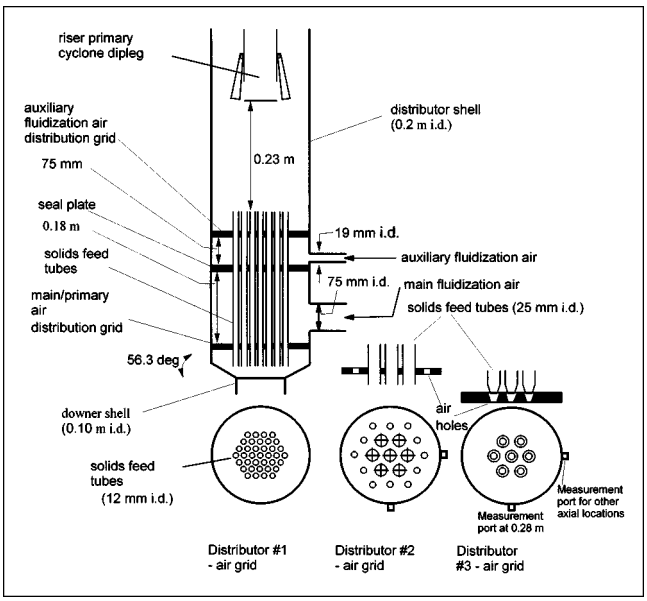

Figure 2. Distributor designs.

being discharged to the storage tank. Any remaining fine particulates are trapped in the baghouse filter.

Three distributor designs, shown in Figure 2, were tested. The distributor shell is a 0.2 m diameter acrylic column attached to the primary cyclone to the conical flanged section that connects to the 0.1 m diameter downer column. The gas and solids distributors were designed as internal of this shell. On top of the auxiliary air distributor grid, a small fluidized bed (operated just above minimum fluidization, approximately 3 cm/s) is formed under the riser primary cyclone dipleg to collect the solids. The solids are then introduced into the top of the downer through 0.36 m long brass tubes that are arranged in an equilateral pitch centered at the downer axis. The solids flow rate is not controlled separately here, but rather by the solids flow in the riser. With increased riser solids fluxes, the height of the fluidized bed in the downer distributor increases, and, subsequently, the flow rate through the downer distributor also increases. The solids circulation rate is measured by diverting the recycled particles to the measuring tank for a given period of time.

Distributor No. 1 (D1) has 37 solids feed tubes (10.7 mm ID and 0.36 m long) with an equilateral pitch length of 19.1 mm. Gas is distributed through a 9.5 mm thick plate with 37 holes (16.7 mm ID) having the same geometrical configuration as the solids feed tubes, located 50.8 mm above the exit of the solids feed tubes. Distributor No. 2 (D2) has seven larger solids feed tubes (25.4 mm ID) with a pitch length of 34.9 mm. Gas is distributed through a 9.5 mm thick acrylic plate with 12 holes (12.7 mm ID) located in the annular region of the column, 50.8 mm above the exit of the solids feed tubes. Gas is thus distributed upstream at the same axial position as with D1 before solids enter the downer, but with a nonuniform gas distribution over the column cross section. The design for D2, as compared to that for D1, was chosen since it constitutes a simple configuration for gas and solids feeding. Distributor No. 3 (D3) is a modification of D2 in which the feed tubes and pitch length are unchanged. Brass fittings of a 12.7 mm length and an internal angle of 70° are pushed onto the bottom of the solids feed tubes. The gas distributor for D3 is characterized by seven nozzles (tapered holes) with the same geometry as the brass conical fittings at the bottom of seven solids feed tubes. The air is then distributed through the gaps formed by the brass fittings and the tapered holes on the gas distribution plate to create a Venturi effect. The vertical location of this plate can be adjusted to vary the nozzle air velocities. With this design, the gas impinges from all directions upon the solids stream exiting from each of the solids feed tubes.

The particulate solids used for this study were fluid cracking catalyst (FCC) particles with a Sauter mean diameter of 67 μm and a particle density of 1,500 kg/m^3. The superficial gas velocity (U_g) (m/s) ranged from 5 to 10 m/s, and the solids fluxes from 43 to 185 kg/m^{2}s. Humidity control by steam injection into the fluidizing air was used to eliminate possible electrostatics in the system.

Measurements of the local solids concentration (ϵ_s) and particle velocity (V_p) (m/s) were taken at 11 radial positions (0.0, 8.1, 19.3, 25.4, 30.0, 34.0, 37.6, 40.9, 43.9, 46.7, and 49.5 mm), using two optical fiber probes. More details about these two probes are given by Zhang et al. (1998) and Zhu et al. (1999b).

Results and Discussion

Measurement results

Visual observations of the solids flow patterns in the near entrance region of the downer show that D1, made up of 37 small diameter feed tubes, provides a stable distribution of solids but distributes a considerable amount of solids near the wall because the 18 tubes in the outer ring of the distributor allow solids to impinge partially on the conical flange connecting the distributor shell to the downer column. D2, made up of seven larger diameter feed tubes, allows the formation of particle jets that are seen to extend to at least 1 to 1.5 m down the column with little or no interaction. D3, a modification of D2 with nozzles, results in dense solids streams located at 2 to 5 cm from the tube ends where the air flow exiting the nozzles converges upon the distributed solids. Different from D2, solids streams formed under D3 break up rapidly and disperse over the column cross section as the air expands.

Figures 3 and 4 provide a direct comparison of typical radial distributions of solids holdup and the radial distributions of particle velocity for D1, D2, and D3. From these figures, it can be observed that the distributor design does not affect the flow patterns in the region far away from the distributors since the ''final'' developed profiles for all three distributors should be very similar for both particle concentration and velocity. However, the distributor design does affect the length of the flow development region. For instance, with solids pre-acceleration in the seven large solids distributor tubes, the flow development length for D2 is around 1.5–2.0 m, much shorter than the lengths for D1 and D3. On the other hand, D3 seems to display a longer distance of flow development than D2, although efforts were made to ensure uniform gas- and solids-distribution and good gas-solids radial mixing at the distributor. It would appear that the nozzle effect has successfully dispersed the solids but also pushed more solids

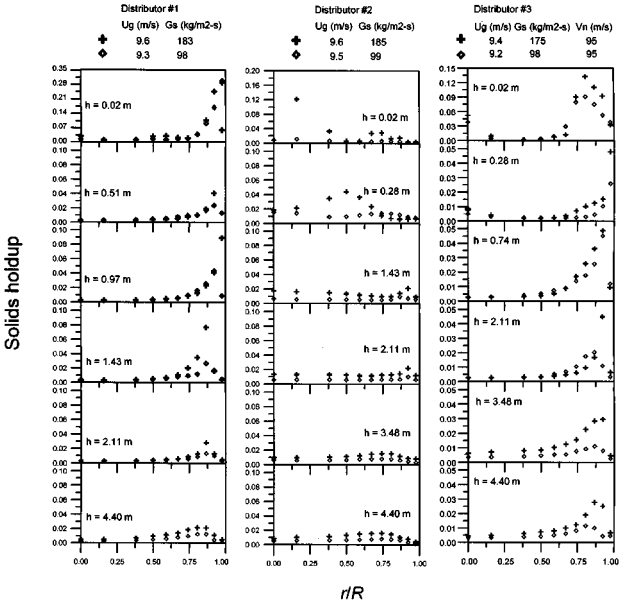

Figure 3. Comparison of radial profiles of solids holdup for D1, D2, and D3.

Y-axis: solids holdup; X-axis: *r/R*.

into the annular region so that a longer distance is necessary for the solids to migrate back into the core. In addition, lower gas velocity through the nozzle in D3 (by lowering the air distributor plate) leads to more uniform radial solids distribution.

Furthermore, the processes of flow development are also different for the three distributors. For D1 and D3, the flow development length is characterized by the distance required for the solids in the annulus to migrate towards the core and for the solids in the annulus to accelerate. The flow development length for D2, however, is characterized by the distance required for the initial dense solids streams to uniformly develop over the column cross section. For D3, the high velocity gas jets significantly alter the solids velocity distributions as compared to D1 and D2. Nozzle-induced flow patterns cause the radial profiles of V_p to develop in a distinctly different manner that is characteristic of the D3 gas and solids distributor.

Figure 5 shows the effect of operating conditions on the radial solids holdup profiles for D1, D2, and D3 at the height of 4.40 m. Increasing G_s leads to more deviations between D1, D2 and D3, while changing U_g does not seem to significantly affect the distribution profiles. The radial solids holdup distribution is more uniform under lower solids circulation rates.

Characterization of flow development

To quantify the flow development analysis, the following radial nonuniformity index (RNI) proposed by Zhu and Manyele (1998), for the solids flow, is used

$$\mathrm{RNI}(\epsilon_s) = \frac{\sigma(\epsilon_s)}{\sigma(\epsilon_s)_{\max}} = \frac{\sigma(\epsilon_s)}{\sqrt{\bar{\epsilon}_s(\epsilon_{s,mf} - \bar{\epsilon}_s)}} \qquad (1)$$

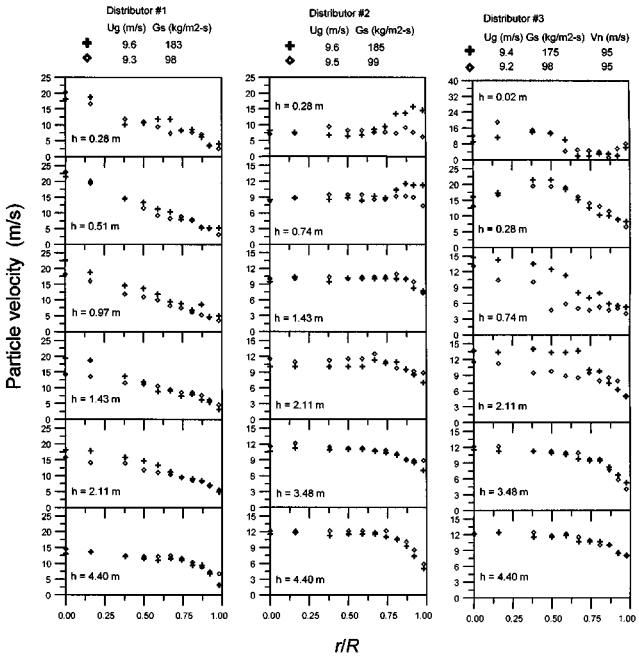

Figure 4. Comparison of radial profiles of particle velocity for D1, D2, and D3.

Y-axis: particle velocity; X-axis: *r/R*.

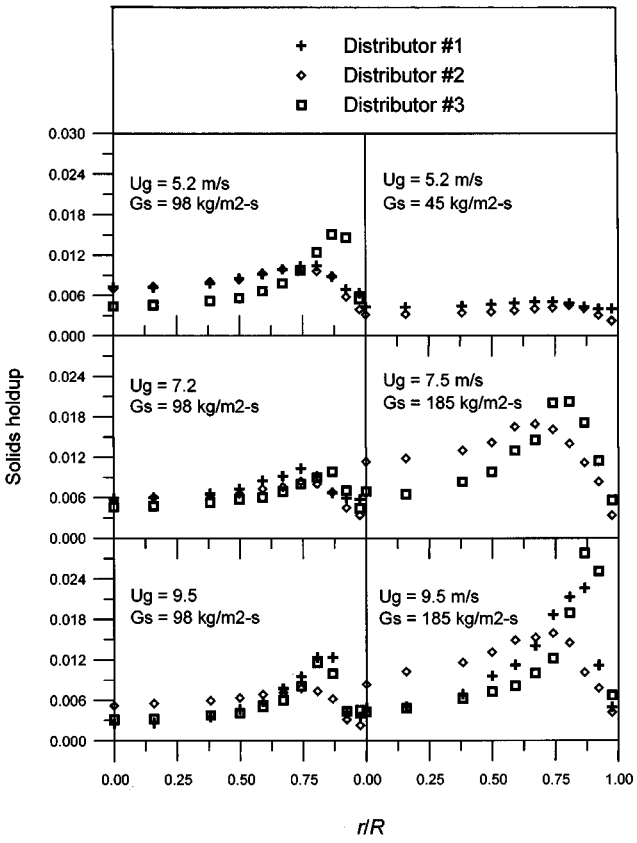

Figure 5. Comparison of radial profiles of solids holdup for D1, D2, and D3 at an axial position of 4.40 m.

Y-axis: solids holdup; X-axis: *r/R*.

where $\sigma(\epsilon_s)$ is the standard deviation of the radial solids holdup profile, $\sigma(\epsilon_s)_{\max}$ is the normalizing parameter, $\bar{\epsilon}_s$ is the cross-sectional average solids holdup, and $\epsilon_{s,mf}$ is the solids holdup at minimum fluidization. RNI(ϵ_s) is actually the normalized standard deviation of the cross-sectional average solids holdup. The normalizing parameter $\sigma(\epsilon_s)_{\max}$ is the maximum possible standard deviation for a particular cross-sectional average solids holdup given that the solids holdup can only have values of either 0 or $\epsilon_{s,mf}$. Therefore, RNI(ϵ_s) must vary between 0 and 1, with larger values indicating more nonuniform flow structures.

Figure 6 provides a comparison of RNI(ϵ_s) as a function of the axial distance from the downer top for the three distributors. A general trend is evident for all three distributors in that the flow becomes more uniform, and the RNI decreases down the column to a constant value. D1 is characterized by large values in the entrance region that gradually decrease to relatively uniform minimum values. This result corresponds to the large solids holdups at the wall and the gradual transition to the fully developed flow. For D2, RNI decreases to a minimum at a height of 2.11 m, but then increases slightly afterwards. This result corresponds to the flattening of the profiles by $h = 1.43-2.11$ m, and then the transition to fully developed flow. For D3, RNI(ϵ_s) oscillates in the top meter of the downer until it begins to gradually decrease towards a stabilized and uniform value. This result corresponds to the asymmetrical nozzle-induced flow patterns in the top of the column, and the subsequent air expansion that entrains the solids to the wall from which they must slowly migrate back to form a uniform radial profile in the developed region.

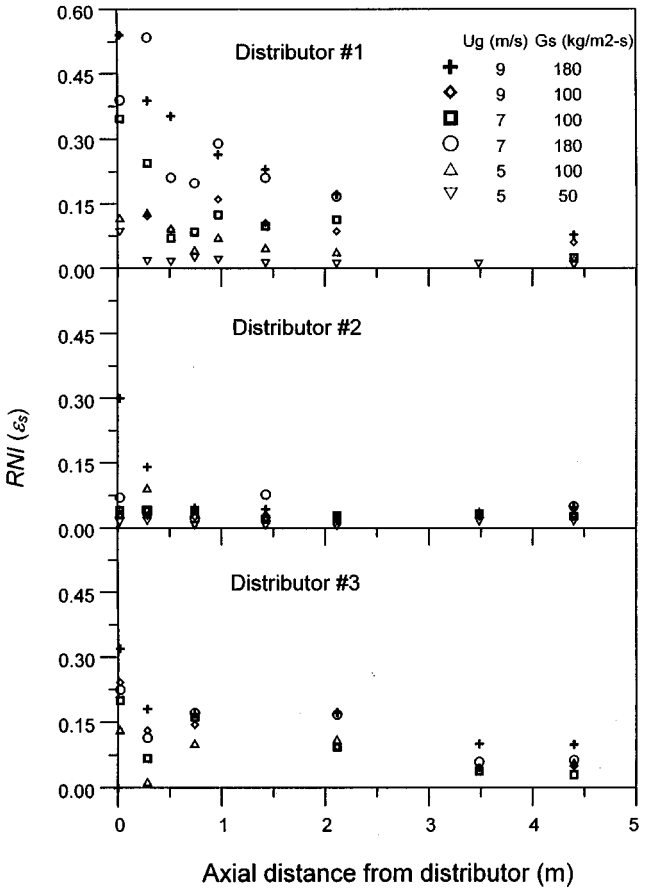

Figure 6. Comparison of axial profiles of RNI(ϵ_s) for D1, D2, and D3.

A similar radial nonuniformity index can also be defined for the particle velocity profiles (Zhu and Manyele, 1998), RNI(V_p)

$$\mathrm{RNI}(V_p) = \frac{\sigma(V_p)}{\sigma(V_p)_{\max}} = \frac{\sigma(V_p)}{\sqrt{(\bar{V}_p - V_{p,\min})(V_{p,\max} - \bar{V}_p)}} \quad (2)$$

Similar to that for RNI(ϵ_s), the normalizing parameter $\sigma(V_p)_{\max}$ represents the maximum possible standard deviation for a particular cross-sectional average particle velocity $\bar{V}_p$ given that the particle velocity can only vary from $V_{p,\min}$ to $V_{p,\max}$. $V_{p,\min}$ is given by the particle velocity for a moving bed under the same solids circulation rate, defined as

$$V_{p,\min} = \frac{G_s}{\rho_p \epsilon_{mf}}. \quad (3)$$

However, the definition of the maximum particle velocity requires more ratiocination. For the RNI(V_p) to provide sensible and normalized comparison, the chosen $V_{p,\max}$ must be higher than the local particle velocities across the column cross section and also vary with the average particle velocity. In the end, the centerline maximum velocity for single-phase laminar flow is used as $V_{p,\max}$, so that

$$V_{p,\max} = 2\bar{V}_p. \quad (4)$$

Again, RNI(V_p) must vary between 0 and 1.

Figure 7 provides a comparison of RNI(V_p) as a function of axial position for the three distributors. Similar trends, as with RNI(ϵ_s), can be observed. The flow becomes more uniform, and the RNI decreases down the column to a constant value. D1 and D3 are characterized by large values of RNI(V_p) in the entrance region that gradually decrease to relatively uniform minimum values. This result corresponds to the larger velocities near the core and the lower velocities near the wall at the entrance, and the subsequent transition to fully developed flow. For D2, RNI approaches a minimum value by a height of about 2 m.

It is clear from Figures 6 and 7 that the two RNIs can be used to characterize the radial flow development and, therefore, can be used to evaluate the effect of the distributor design on the downer flow. For example, the magnitude of change in RNIs from the entrance to the developed regions is greater for a larger G_s. In addition, both RNI(ϵ_s) and RNI(V_p) for the three different distributors are found to approach the similar values in the lower region away from the distributor, indicating that the effect of the distributor design is only limited to the entrance region. Moreover, for a lower G_s, this final minimum value is approached more rapidly. This outcome is justified since lower G_s promotes rapid flow development.

Although the fully developed radial flow distribution in the downer is much more uniform than that in the riser, the flow

development length for the downer seems to be comparable with the riser, extending several meters into the downer column from the gas and solids distributor under different operating conditions (Figures 6 and 7). However, the actual time needed for the flow to develop is much shorter in the downer given the more rapid particle acceleration. In addition, the radial flow structures in the developing region of the downer are more uniform than those in the developing region of the riser, and, in most cases, also more uniform than the fully developed radial structures in the riser (Lim et al., 1995).

Both the superficial gas velocity and the solids circulation rate were found to affect the hydrodynamics inside the downer (Figures 6 and 7). Increases of the solids circulation rate tend to increase the length for flow development, because the extra solids require longer distances to disperse uniformly. Contrary to what has been observed in the riser, the superficial gas velocity in the downer appears to have a lesser effect on the development of the radial profiles, probably because the particle acceleration momentum mainly comes from the gravitational force rather than from the gas flow. Furthermore, increasing the gas velocity in the downer leads to slight increases of the acceleration length since the ''final'' particle velocity is higher (Zhang et al., 1999). Again, this result is different as compared to the riser where increasing the gas velocity will reduce the particle acceleration length.

General guidelines for downer distributor design

Operations with three different distributor designs shows (Figures 3, 4, 6 and 7) distinctly different radial flow patterns as the solids holdup and particle velocity profiles develop. D1, with evenly distributed gas and solids flow in the core region but larger solids flow in the annular region, leads to larger solids holdups near the wall. D2, with larger solids distributor tubes which allow solids pre-acceleration, leads to a more uniform radial solids distribution. D3, with air jetting into the solids feed streams, does not seem to enhance, but, rather to somewhat impede, the radial flow development. This is probably because the gas jets disperse more particles into the wall region where particle acceleration is hindered by the wall effect. Therefore, as far as solids flow development is concerned, D2 seems to give the best results since: (1) it distributes most of the solids away from the wall; (2) it allows solids pre-acceleration inside the large distribution tubes. D3 is better than D1, but not as good as D2, as shown clearly by the two RNIs. The distribution of gas seems to be less important to the flow development in the downer since it is the gravity which acts as the main driving force for solids acceleration. From the observations of D2, which distributes gas predominantly in the annular region of the column, it may even be suggested that higher initial gas velocities near the wall may dilute the solids flows in the annular region and minimize solids-wall friction.

However, rapid solids flow development is not the only parameter which characterizes a good downer distributor. More importantly, quick and effective gas-solids initial radial mixing must be facilitated to ensure uniform reaction times inside the downer. Given the expected short reaction times, rapid gas-solids radial mixing is much more critical as a design parameter in the downer than in the riser. In this case,

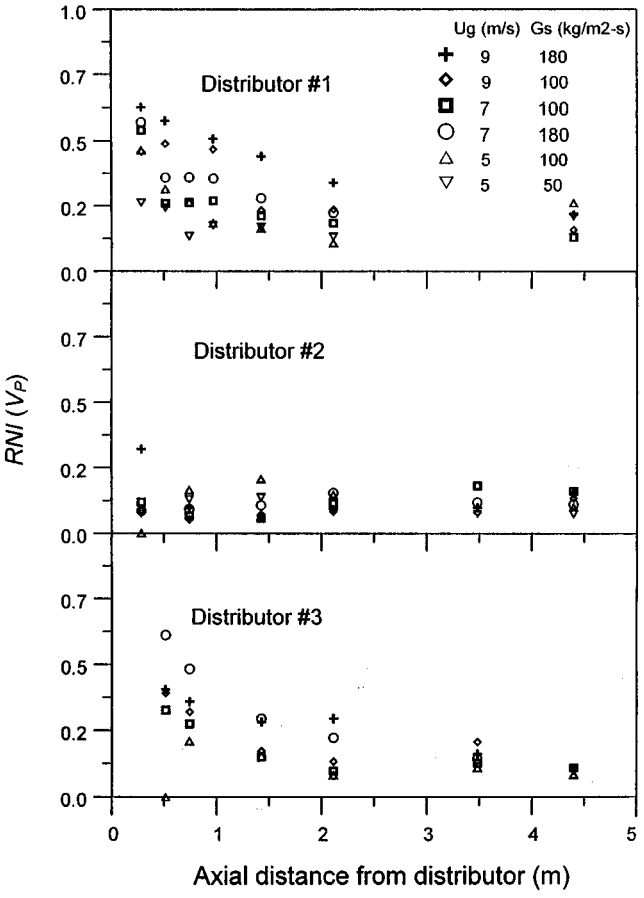

Figure 7. Comparison of axial profiles of RNI(V_p) for D1, D2, and D3.

D2 would not be a good choice since separate gas and solids distributions lead to masses of dense and high velocity particle jets that persist down the column and impede initial gas-solids mixing. On the other hand, D3 is shown to be the best choice given its nozzle design which forces the gas to thoroughly contact the solids streams (Zhu et al., 1999a). D1 provides a more even distribution of gas and solids, if not considering the overloading of solids near the wall, and would also be a better design than D2.

Therefore, good downer distributor design practice must consider both the initial gas-solids mixing and the gas- and solids-flow development. The gas and solids distribution must both enable rapid flow development and enhance gas-solids contacting (interaction). An optimal downer distributor will provide an even distribution of pre-accelerated solids, and an even distribution of gas from high velocity gas nozzles that impart large momentum upon the solids, thereby improving flow development, maximizing acceleration, and enhancing solids dispersion and gas-solids mixing over the column cross section. This ideal design will ensure uniform products from fast chemical reactions to be potentially conducted in downer reactors. A large number of small diameter and evenly spaced solids feed tubes are required to provide a constant flow of particles from the individual tubes and, therefore, even solids distributions over the column cross section. Solids should not be distributed near the column wall, because the radial

movement of particles from this region is slow so that the nonuniformity of solids holdup can persist over large distances. The increased wall friction is detrimental to both solids acceleration and flow development. Nozzles are very important tools for enhancing gas-solids mixing, and should be utilized wherever possible. Additionally, erosion of column walls and any hardware inserts is rapid. Inserts, such as the side-jets used by Wei et al. (1996), should be avoided.

Conclusions

The effects of the gas- and solids-distributor design and the operating conditions on the development of the flow structure in a gas-solids pilot-scale, cold model downer reactor were studied using FCC particles and three different distributor designs. The local solids holdups and particle velocities were measured using two separate fiber optic sensors. The hydrodynamics inside the downer are affected by both the operating conditions and the distributor designs. The superficial gas velocity appears to extend the flow development length, but, unlike in the riser, does not seem to affect the shapes of the radial flow profiles in the developing region. Decreasing the solids circulation rate, however, tends to decrease the flow development length. The distributor design is very critical to the initial flow structure development in the downer. Even in this type of relatively homogeneous gas-solids contactor, the flow development length in the downer is rather long if the distributor design is inappropriate. To maximize the potential of the downer, the optimal distributor should provide an even distribution of gas from high velocity gas nozzles that impart large momentum upon the solids, thereby improving flow development and solids dispersion, and maximizing solids acceleration and gas-solids mixing. The solids should be distributed away from the column wall because dense solids flow at the wall can persist for large distances. A large number of small diameter and evenly spaced solids feed tubes away from the wall will provide a constant flow of particles from each tube and, therefore, an even solids distribution over the column cross section.

Acknowledgments

The authors are grateful to the National Sciences and Engineering Research Council (NSERC) for its financial support of this project. The authors would also like to express thanks to Jeff Ball and Ying Ma for their support and assistance in collecting the experimental data.

Notation

G_s = solids circulation rate, kg/m^{2}s
h = axial distance from the bottom end of solids feed tubes at the downer entrance
r/R = normalized radial position
RNI(ϵ_s) = radial nonuniformity index for solids concentration, RNI(ϵ_s) = $\sigma(\epsilon_s)/\sigma(\epsilon_s)_{\max}$
RNI(V_p) = radial nonuniformity index for particle velocity, RNI(V_p) = $\sigma(V_p)/(V_p)_{\max}$
V_n = nozzle velocity for distributor No. 3, m/s
$\bar{V}_p$ = cross-sectional average particle velocity, m/s
$\epsilon_{s,mf}$ = solids holdup at minimum fluidization
ρ_p = particle density, kg/m^3
$\sigma(V_p)$ = standard deviation of radial particle velocity distribution
$\sigma(V_p)_{\max}$ = maximum possible standard deviation for a particular radial V_p profile given that the solids holdup can only vary from $V_{p,\min}$ to $V_{p,\max}$

Literature Cited

Bai, D.-R., Y. Jin, Z.-Q. Yu and N.-J. Gan, "Radial Profiles of Local Solid Concentration and Velocity in a Concurrent Downflow Fast Fluidized Bed," *Circulating Fluidized Bed Technology III*, P. Basu, M. Horio, and M. Hasatani, eds., Pergamon Press, Toronto, p. 157 (1991).

Gross, B., and M. P. Ramage, "FCC Reactor with a Downflow Reactor Riser," U.S. Patent No. 4,385,985 (1983).

Gross, B., "Heat Balance in FCC Process and Apparatus with Downflow Reactor Riser," U.S. Patent No. 4,411,773 (1983).

Herbert, P. M., T. A. Gauthier, C. L. Briens, and M. A. Bergougnou, "Application of Fiber Optic Reflection Probes to the Measurement of Local Particle Velocity and Concentration in Gas-Solid Flow," *Powder Technol.*, **80**, 243 (1994).

Herbert, P. M., "Hydrodynamic Study of a Downflow Circulating Fluidized Bed," PhD Diss., The University of Western Ontario, London, Canada (1997).

Lim, K. S., J.-X. Zhu, and J. R. Grace, "Hydrodynamics of Gas-Solid Fluidization," *Int. J. Multiphase Flow*, **21**(Suppl.), 141 (1995).

Mirgain, C., C. L. Briens, M. del Pozo, R. Loutaty, and M. A. Bergougnou, "Experimental Evaluation of Gas-Solids Mixing Chambers for Short Contact Times Fluidized Bed Reactors," *Fluidization IX*, L.-S. Fan and T. M. Knowlton, eds., Engineering Foundation, New York, p. 357 (1998).

Niccum, P. K., and D. P. Bunn, "Catalytic Cracking System," U.S. Patent No. 4,514,285 (1985).

Sobocinski, K., B. Young, and H. I. de Lasa, "New Fibre Optic Method for Measuring Velocities of Strands and Solids Hold-Ups in Gas-Solid Downflow Reactors," *Powder Technol.*, **83**, 1 (1995).

Wang, Z., D. Bai, and Y. Jin, "Hydrodynamics of Cocurrent Downflow Circulating Fluidized Bed (CDCFB)," *Powder Technol.*, **70**, 271 (1992).

Wei, F., Z.-W. Wang, Y. Jin, Z.-Q. Yu, and W. Chen, "Dispersion of Lateral and Axial Solids in a Cocurrent Downflow Circulating Fluidized Bed," *Powder Technol.*, **81**, 25 (1994).

Wei, F., Y. Jin, Z.-Q. Yu, and J.-Z. Liu, "The Gas Mixing in Cocurrent Downflow Circulating Fluidized Bed," *Chem. Eng. and Technol.*, **18**, 59 (1995).

Wei, F., and J.-X. Zhu, "Effect of Flow Direction on the Solids Mixing in Gas-Solids Upflow and Downflow Systems," *Chem. Eng. J.*, **64**, 345 (1996).

Wei, F., J. Liu, Y. Jin, and Z. Yu, "Hydrodynamics and Mixing Behaviors in the Entrance Region of a Downer," *Circulating Fluidized Bed V*, M. Kwauk and J. Li, eds., AIChE, New York, p. 122 (1996).

Wirth, K.-E., and T. Schiewe, "Flow Structures in a Downer Reactor," *Fluidization IX*, L.-S. Fan and T. M. Knowlton, eds., Engineering Foundation, New York, p. 253 (1998).

Zhang, H., P. M. Johnston, J.-X. Zhu, H. I. de Lasa, and M. A. Bergougnou, "A Novel Calibration Procedure for a Fibre Optic Concentration Probe," *Powder Technol.*, **100**, 260 (1998).

Zhang, H., J.-X. Zhu, and M. A. Bergougnou, "Flow Development in a Gas–Solids Downer Fluidized Bed," *Can. J. Chem. Eng.*, **77**, 194 (1999).

Zhu, J.-X., Z.-Q. Yu, Y. Jin, J. R. Grace, and A. Issangya, "Cocurrent Downflow Circulating Fluidized Bed (Downer) Reactors—A State of the Art Review," *Can. J. Chem. Eng.*, **73**, 662 (1995).

Zhu, J.-X., and F. Wei, "Recent Developments of Downer Reactors and Other Types of Short Contact Reactors," *Fluidization VIII*, J. F. Large and C. Laguerie, eds., Engineering Foundation, New York, p. 501 (1996).

Zhu, J.-X., and S. V. Manyele, "Radial Non-Uniformity Index (RNI) in Fluidized Beds and Multiphase Flow Systems," 48th Can. Chem. Eng. Conf., London, Canada (Oct. 4–7, 1998).

Zhu, J.-X., Y. Ma. and H. Zhang, "Gas-Solids Contact Efficiency in the Entrance Region of a Co-Current Downflow Fluidized Bed (Downer)," *Chem. Eng. Res. Dev.*, **77**, 151 (1999a).

Zhu, J.-X., S. Qin, G. Li, F. Li, H. Zhang, Y. L. Yang, and J. R. Grace, "Direct Measurements of Particle Velocity in Gas-Solids Suspension Flow using a Novel 5-Fibre Optical Probe," *Powder Technol.*, in press (1999b).

Manuscript received Mar. 16, 1998, and revision received April 20, 1999.